Electronic Supplementary Material (ESI) for ChemComm.

Supporting information

Near-Infrared in Vivo Bioimaging by Upconversion Molecular Probe

Yi Liu,† Qianqian Su,† Xianmei Zou, Min Chen, Wei Feng, Yibing Shi, Fuyou Li*

Department of Chemistry & The State Key Laboratory of Molecular Engineering of Polymers & Institute of Biomedicine Science, Fudan University, Shanghai, 200433, P. R. China.

Supporting information

Experimental Procedures

Materials: All reagents and chemicals were purchased from commercial sources and used without further purification. 2,3,3-trimethyl-3H-indolium, ethyliodide, triethyl orthoformate, cyclohexanone, N,N'-bisphenylformamidine and 2-(4-diethylamino-2-hydroxybenzoyl)benzoic acid were used without further purification. Ac_2O, ethanol and toluene were obtained from Alfa Aesar Ltd. Rare earth oxides Y_2O_3 (99.999%), Yb_2O_3 (99.999%), Nd_2O_3 (99.999%) and Er_2O_3 (99.999%) were purchased from Shanghai Yuelong New Materials Co. Ltd. $RECl_3$ (RE^{3+} = Y^{3+}, Yb^{3+}, Nd^{3+}, and Er^{3+}) were prepared with the literature method. Ethanol and deionized water was used to prepare all aqueous solutions. The amphiphilic block-polymer poly(maleic anhydride-alt-1-octadecene)-PEG (pPEG) was prepared according to the previous literatures.

Characterization. The ^1H and ^{13}C NMR spectra were recorded on a Bruker spectrometer at 400 MHz. All chemical shifts are reported in the standard δ notation of parts per million (ppm). Matrix assisted laser desorption ionization-time of flight mass spectra (MALDI-TOF-MS) were measured on an AB SCIEX 5800 system. UV-Vis absorption spectra were recorded on a Shimadzu 3000 spectrophotometer. Upconversion luminescence (UCL) emission spectra were measured on an Edinburgh FLS920 luminescence spectrometer with an external 1.5 W adjustable 808 nm semiconductor laser (Beijing Hi-Tech Optoelectronic Co., China). In our case, all power densities of CW 808 nm excitation for the UCL measurements were fixed at 1.0 W cm^{-2}. FT-IR spectra were measured using an IR Prestige-21 spectrometer (Shimadzu) from samples in KBr pellets. X-ray powder diffraction (XRD) measurements were performed on a Bruker D8 diffractometer at a scanning rate of 1° min^{-1} in the 2θ range of 10−90°, with graphite

monochromated Cu Kα radiation (λ = 1.5406 nm). TEM images were collected on a JEM 2010 operating at an acceleration voltage of 200 kV. The as-prepared samples were dispersed in cyclohexane or water and dripped onto a copper grid for the TEM tests. X-ray computed tomography (X-ray CT) images was carried out on a high resolution in vivo micro-CT imaging system (SkyScan 1176, Beckman Coulter)

Synthetic procedure to NIR dye NRh-1

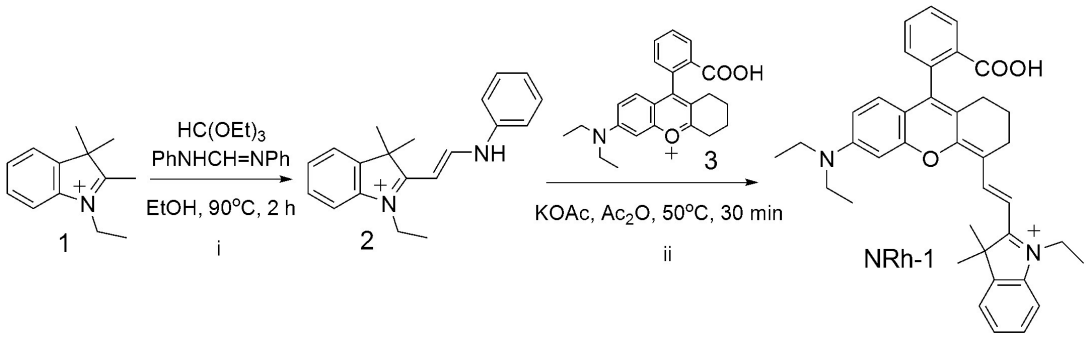

Scheme S1. Chemical structure and synthetic route to NRh-1.[a]

[a] Reagents and conditions: (i) triethyl orthoformate, N,N'-bis-phenylformamidine, ethanol, 90 ˚C, 95%; (ii) KOAc, Ac_2O, 50 ˚C, 70%.

Typical procedure for the synthesis of compound 1. A solution containing 2,3,3-trimethyl-3H-indolium (50 mmol), ethyliodide (50 mmol), and toluene (50 mL) were heated at 110 ˚C for 24 h. The mixture was then cooled down to room temperature followed by the addtion of 200 mL dry diethyl ether for the formation of compound 1. The resulting product was isolated by filtration under reduced pressure, washed with ice-cold diethyl ether, and then dried in a freeze drying apparatus.[1] The yield was 96%. ^{1}H NMR (400 MHz, $CDCl_3$) δ 7.75 – 7.66 (m, 1H), 7.66 – 7.55 (m, 3H), 4.79 (q, J = 7.4 Hz, 2H), 3.17 (s, 6H), 1.67 (s, 6H), 1.63 (t, J = 7.4 Hz, 3H).; MS (MALDI-TOF-MS): calcd for $C_{13}H_{18}N^+$, 188.1 $[M]^+$; found, 188.1 $[M]^+$.

Typical procedure for the synthesis of compound 2: 1-Ethyl-2,3,3-trimethyl-3H-indolium bromide (10 mmol), triethyl orthoformate (10 mmol), and N,N'-bis-phenylformamidine (10 mmol) were dissolved in 6 mL ethanol. The mixture was then heated under reflux for 2 h. The resulting solution was subsquently cooled down to room temperature and then poured into ice water. The as-prepared product was isolated by filtration under reduced pressure, washed with ice-cold diethyl ether, and then dried in a freeze drying apparatus. The compound 2 (95% in yield) obtained as orange crystals in 95% yield.[2] ^{1}H NMR (400 MHz, d_6-DMSO) δ 11.89 (s, 1H), 8.65 (d, J = 12.4 Hz, 1H), 7.67 (d, J = 7.2 Hz, 1H), 7.53 (t, J = 7.0 Hz, 1H), 7.50 – 7.45 (m, 4H), 7.33 (t, J = 7.4 Hz, 1H), 7.30 – 7.25 (m, 1H), 6.16 (d, J = 11.5 Hz, 1H), 4.15 (q, J = 7.1 Hz, 2H), 1.69 (s, 6H), 1.33 (t, J = 7.2 Hz, 3H).; MS (MALDI-TOF-MS): calcd for $C_{20}H_{23}N_2^+$, 291.2 $[M]^+$; found, 291.3 $[M]^+$.

Typical procedure for the synthesis of compound 3: Freshly distilled cyclohexanone (6.6 ml, 63.7 mmol) was added dropwise to concentrated H_2SO_4 (70 mL). The resulting solution was then cooled down to 0 ˚C. Then 2-(4-diethylamino-2-hydroxybenzoyl)benzoic acid (10 g, 32 mmol) was added in portions over a period of 30 min under vigorous stirring. The reaction mixture was heated to 90 ˚C and kept for 1.5 h before cooling down to room temperature. The resulting mixture was poured into ice (300 g). 70% perchloric acid (7 ml) was then added to the as-obtained solution. The precipitate was filtered off, and washed with cold water (100 mL). The red cruder product in 90% yield was collected without further purification.[3] ^{1}H NMR (400 MHz, CD_3CN) δ 8.27 (d, J = 7.9 Hz, 1H), 7.84 (t, J = 7.5 Hz, 1H), 7.75 (t, J = 7.7 Hz, 1H), 7.23 (d, J = 7.6 Hz, 1H), 7.16 (dd, J = 9.7, 2.2 Hz, 1H), 7.11 (s, 1H), 6.96 (d, J = 2.1 Hz, 1H), 3.63 (q, J = 7.2 Hz, 4H), 3.15 – 2.97 (m, 2H), 2.22 (t, J = 6.0 Hz, 2H), 1.92 (dd, J = 11.7, 5.4 Hz, 2H), 1.74

(dd, *J* = 11.7, 5.7 Hz, 2H), 1.25 (t, *J* = 7.0 Hz, 6H).; MS (MALDI-TOF-MS): calcd. For $C_{24}H_{26}NO_3^+$ 376.2 $[M]^+$; found 376.3 $[M]^+$.

Typical procedure for the synthesis of NRh-1: The freshly prepared compound **2** (2.0 mmol), compound **3** (2.0 mmol) and KOAc were dissolved in an Ac_2O solution (15 mL). The mixture was heated at 50 ˚C until the solution turned green. The mixture was then poured into 100 mL water solution under vigorous stirred for 10 min at RT. The crude product was filtered, washed exhaustively with water and ethyl ether for 3 times. The as-synthesized NRh-1 was then purified by silica column chromatography using DCM/MeOH (v/v, 40:1) mixture as eluent. The green fraction was collected. The yield was 70%. ^{1}H NMR (400 MHz, CD_3OD) δ 8.65 (d, *J* = 13.7 Hz, 1H), 8.10 (d, *J* = 6.9 Hz, 1H), 7.64 – 7.57 (m, 2H), 7.53 (d, *J* = 7.3 Hz, 1H), 7.40 (d, *J* = 7.6 Hz, 1H), 7.31 – 7.24 (m, 2H), 7.18 (d, *J* = 7.1 Hz, 1H), 6.87 (d, *J* = 9.1 Hz, 1H), 6.79 (d, *J* = 8.9 Hz, 1H), 6.72 (s, 1H), 6.15 (d, *J* = 14.0 Hz, 1H), 4.17 (d, *J* = 7.0 Hz, 2H), 3.56 (d, *J* = 6.9 Hz, 4H), 3.18 (dd, *J* = 14.6, 7.3 Hz, 2H), 2.67 (d, *J* = 10.6 Hz, 2H), 2.44 – 2.34 (m, 2H), 1.63 – 1.54 (m, 2H), 1.41 (t, *J* = 6.7 Hz, 3H), 1.24 (d, *J* = 6.9 Hz, 6H). ^{13}C NMR (101 MHz, CD_3OD) δ 171.74, 163.46, 156.11, 155.07, 152.20, 141.99, 141.13, 140.86, 134.66, 130.58, 128.60, 124.49, 122.12, 120.86, 115.39, 113.81, 112.25, 110.08, 97.89, 95.13, 44.63, 38.60, 27.37, 26.42, 23.87, 20.38, 11.40, 10.87, 7.83. MS (MALDI-TOF-MS): calcd. For $C_{38}H_{42}N_2O_3^+$ 573.3 $[M]^+$; found 573.4 $[M]^+$.

Synthesis of oleic acid (OA)-coated $NaYF_4$:Yb,Er,Nd nanoparticle (OA-UCNPs). OA-UCNPs were prepared by a modified solvothermal process.[4] YCl_3 (0.685 mmol), $YbCl_3$ (0.300 mmol), $NdCl_3$ (0.010 mmol), and $ErCl_3$ (0.005 mmol) were mixed with 6 mL oleic acid and 15 mL octadecene in a 100 mL flask. The solution was heated to 160°C to form a homogeneous

solution, and then cooled to room temperature. Methanol solution (8 mL) containing NaOH (2.5 mmol) and NH_4F (4 mmol) was added slowly to the flask and stirred for 30 min. The solution was heated slowly and degassed at 120°C for 10 min to remove the methanol, and then heated to 300°C and maintained for 1 h under Ar. After the solution had cooled naturally, nanoparticles were precipitated from the solution with EtOH, washed with EtOH/cyclohexane (9:1, v/v) three times, and finally redispersed in 10 mL of cyclohexane.

Synthesis of OA-coated $NaYF_4$:Yb,Er,Nd@$NaYF_4$:Nd core-shell nanocomposite (OA-csUCNPs:Nd). csUCNPs:Nd was prepared by a modified solvothermal process.[4] YCl_3 (0.80 mmol) and $NdCl_3$ (0.20 mmol) were mixed with 6 mL oleic acid and 15 mL octadecene in a 100 mL flask. The solution was heated to 160°C to form a homogeneous solution, and then cooled to room temperature. The as-synthesized $NaYF_4$:Yb,Er,Nd nanoparticles in 5 mL of cyclohexane were added, and the mixture was stirred at 60°C for 30 min. A methanol solution (8 mL) containing NaOH (2.5 mmol) and NH_4F (4 mmol) was added slowly into the flask and stirred for 30 min. The solution was heated slowly and degassed at 120°C for 10 min to remove methanol, and then heated to 300°C and maintained for 1 h under Ar. After the solution had cooled naturally, nanoparticles were precipitated from the solution with ethanol, and washed with ethanol/cyclohexane (9:1, v/v) three times.

Synthesis of pPEG-modified csUCNPs:Nd nanocomposite (pPEG-csUCNPs:Nd). pPEG-csUCNPs:Nd was prepared according to a previous method.[5] The OA-csUCNPs:Nd (10 mg) was dispersed in 5 mL chloroform by ultrasonication, and the mixture was stirred at room temperature to obtain a homogeneous phase. The amphiphilic polymer (pPEG, 10 mg) was added, and the mixture was stirred overnight at room temperature. The mixture was centrifuged

(14000 rpm, 8 min, 20°C), and the collected solid was washed repeatedly with water. The precipitate could be redispersed in deionized water.

Synthesis of csUCNPs:Nd nanocomposite modified with pPEG and NRh-1 (NRh-1-csUCNPs:Nd). The synthesis procedure for NRh-1-csUCNPs:Nd is similar to that of pPEG-csUCNPs:Nd, but the reagents NRh-1 (2 mg), pPEG (10 mg) and OA-csUCNPs:Nd (10 mg) were used.

Cell Culture. The cell lines HeLa and KB were provided by the Institute of Biochemistry and Cell Biology, SIBS, CAS (China). The HeLa and KB cells were grown in modified Eagle's medium supplemented with 10% fetal bovine serum at 37 ˚C and 5% CO_2. HeLa and KB cells were planted on 14 mm glass coverslips and allowed to adhere for 24 h.

Cytotoxicity of NRh-1 and NRh-1-csUCNPs:Nd.[5] *In vitro* cytotoxicity was measured by performing MTT assays on the HeLa and KB cells. Cells were seeded into a 96-well cell culture plate at 5×10^4/well, under 100% humidity, and were cultured at 37 ˚C and 5 % CO_2 for 24 h; the different concentrations of NRh-1 (0, 10, 20, 30, 40, 60 and 80 μM, diluted in RPMI 1640) and NRh-1-csUCNPs:Nd (0, 100, 200, 300, 400, 500, and 600 μg/mL, diluted in RPMI 1640) were then added to the wells. The cells were subsequently incubated for 24 h at 37 ˚C under 5 % CO_2. Then, MTT (10 mL; 5 mg/mL) was added to each well, and the plate was incubated for an additional 4 h at 37 ˚C under 5% CO_2. After the addition of 100 μL DMSO, the assay plate was allowed to stand at room temperature for 2 h. The optical density OD570 value (Abs) of each well, with background subtraction at 690 nm, was measured by means of a Tecan Infinite M200 monochromator-based multifunction microplate reader. The following formula was used to calculate the inhibition of cell growth:

cell viability(%) = (mean Abs value of treatment group/mean Abs value of control) ×100%

Upconversion luminescence bioimaging *in vivo* and *ex vivo*.[6] The animal procedures were in agreement with the guidelines of the Institutional Animal Care and Use Committee. To conduct the UCL bioimaging, the UCL *in vivo* imaging system was built. One external 0–1.5 W adjustable CW 808 nm semiconductor laser was used as excitation source, and a cooled electron-multiplying charge-coupled device (Andor DU897) was used as the signal collector. After the subcutaneous injection of NRh-1 and NRh-1-csUCNPs:Nd, UCL imaging *in vivo* was performed. For lymphatic imaging, 20 μL NRh-1-csUCNPs:Nd was injected intradermally into the foreclaw. At 30 min postinjection, UCL lymphatic imaging *in vivo* was performed under excitation at 808 nm. For intragastric administration imaging, 0.1 mL NRh-1-csUCNPs:Nd was injected intragastrically, UCL imaging *in vivo* was performed at 5 min postinjection. For the biodegradability experiment, NRh-1 and NRh-1-csUCNPs:Nd were injected intravenously into the mice, and UCL imaging was conducted at different times. UCL emissions at 514–560 nm (green channel), 635–680 nm (red channel), and 680–750 nm (NIR channel) were collected using a band-pass filter.

Signal-to-noise ratio (SNR) = [(mean luminescence intensity of region 1) − (mean luminescence intensity of region 3)]/[(mean luminescence intensity of region 2) − (mean luminescence intensity of region 3)].

Absolute photoluminescence quantum yields (Φ). The absorption and luminescence measurements were performed with air-saturated freshly prepared dye solution at 25 ˚C using 10 × 10 mm quartz cuvettes. Absolute Φ values were determined with the integrating sphere.

The following formula was used to calculate the absolute $\Phi_{internal}$ and $\Phi_{external}$ values:

$$\Phi_{internal} = \frac{N_{em(sample)}}{N_{ex(blank)} - N_{ex(sample)}}$$

$$\Phi_{external} = \frac{N_{em(sample)}}{N_{ex(sample)}}$$

$N_{em(sample)}$, $N_{ex(blank)}$ and $N_{ex(sample)}$ stand for the number of the emitted photons in sample, the excited photons in blank and the excited photons in sample.

Table S1. The photoluminescence quantum yields of NRh-1.

Stokes	$\boldsymbol{\Phi_{internal}}$	7.24% (λ_{ex}=670 nm)
	$\boldsymbol{\Phi_{external}}$	4.71% (λ_{ex}=670 nm)
Anti-Stokes	$\boldsymbol{\Phi_{internal}}$	1.82% (λ_{ex}=808 nm)
	$\boldsymbol{\Phi_{external}}$	1.36 ‰ (λ_{ex}=808 nm)

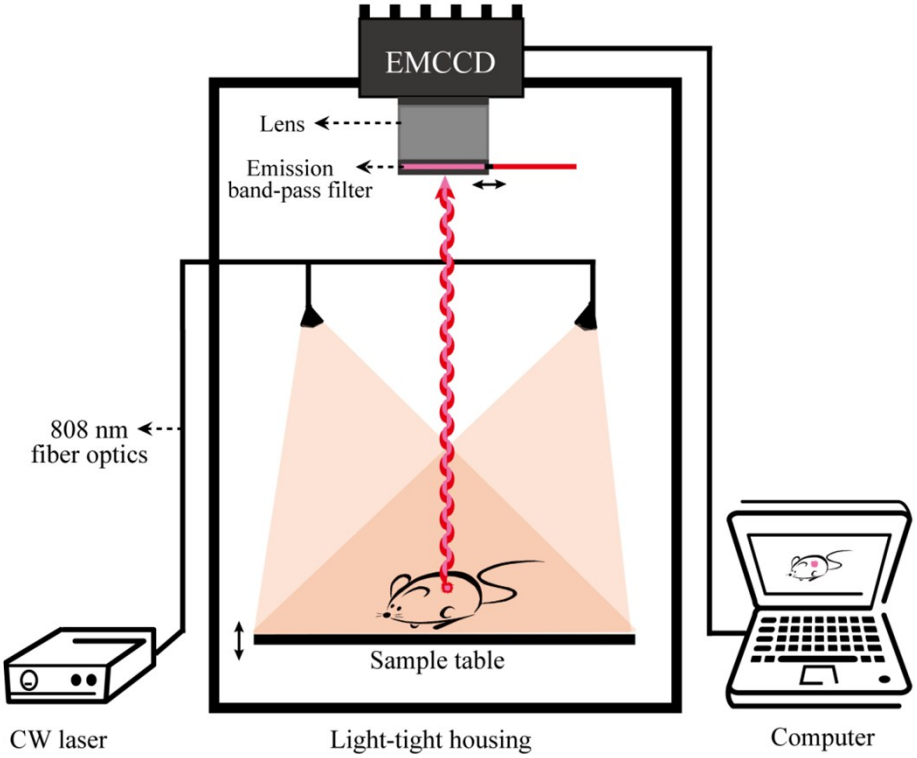

Scheme S2. Diagram depicting the experimental setup for the small-animal upconversion luminescence imaging system.

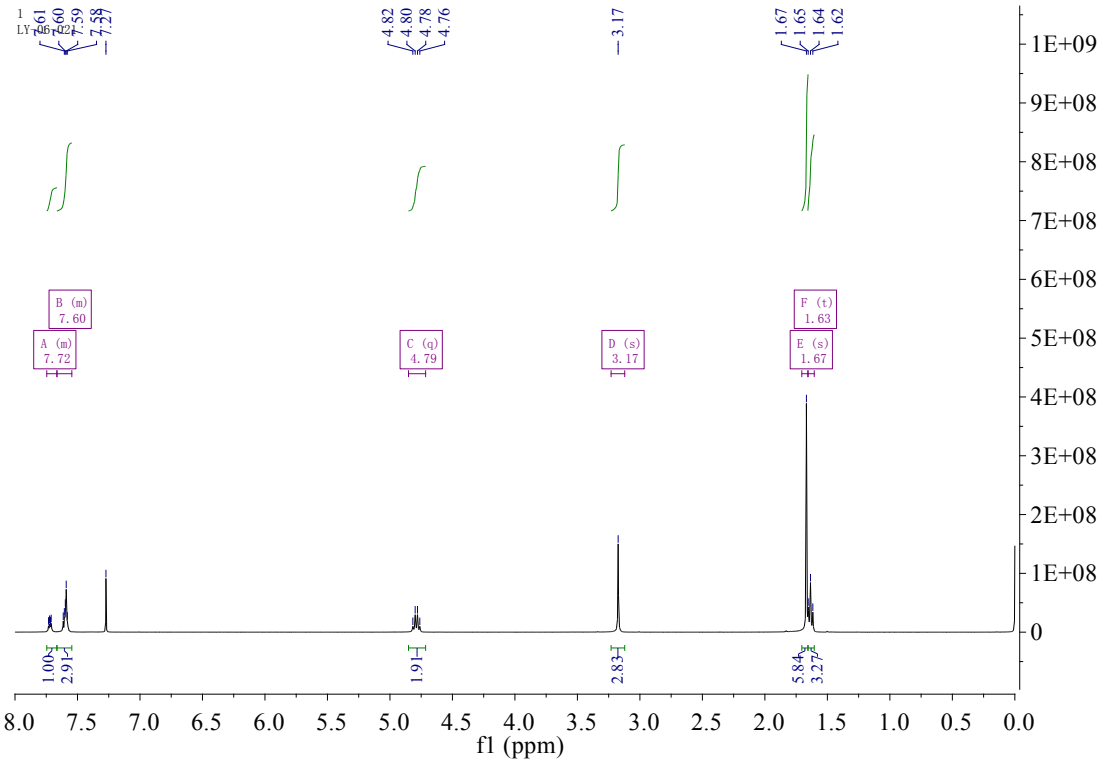

Figure S1. ^{1}H NMR spectrum for compound **1**.

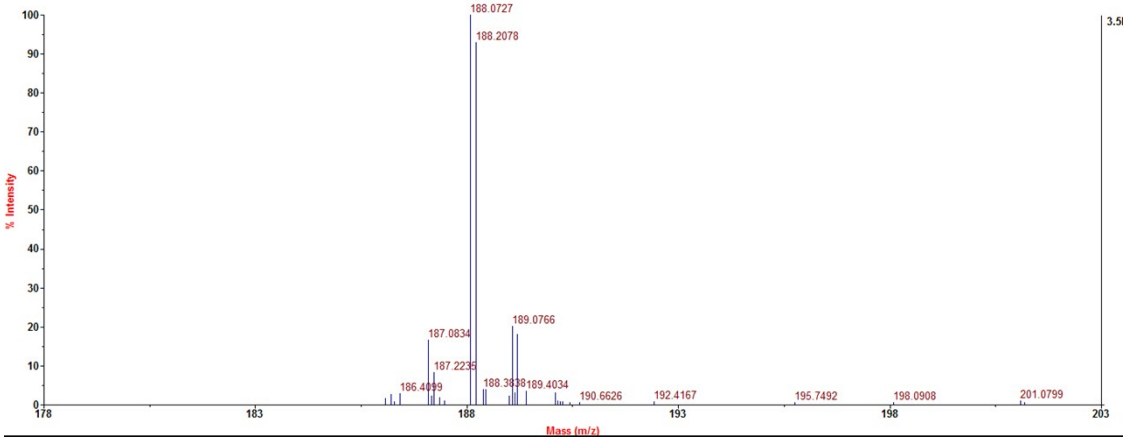

Figure S2. MALDI-TOF-MS spectrum for compound **1**.

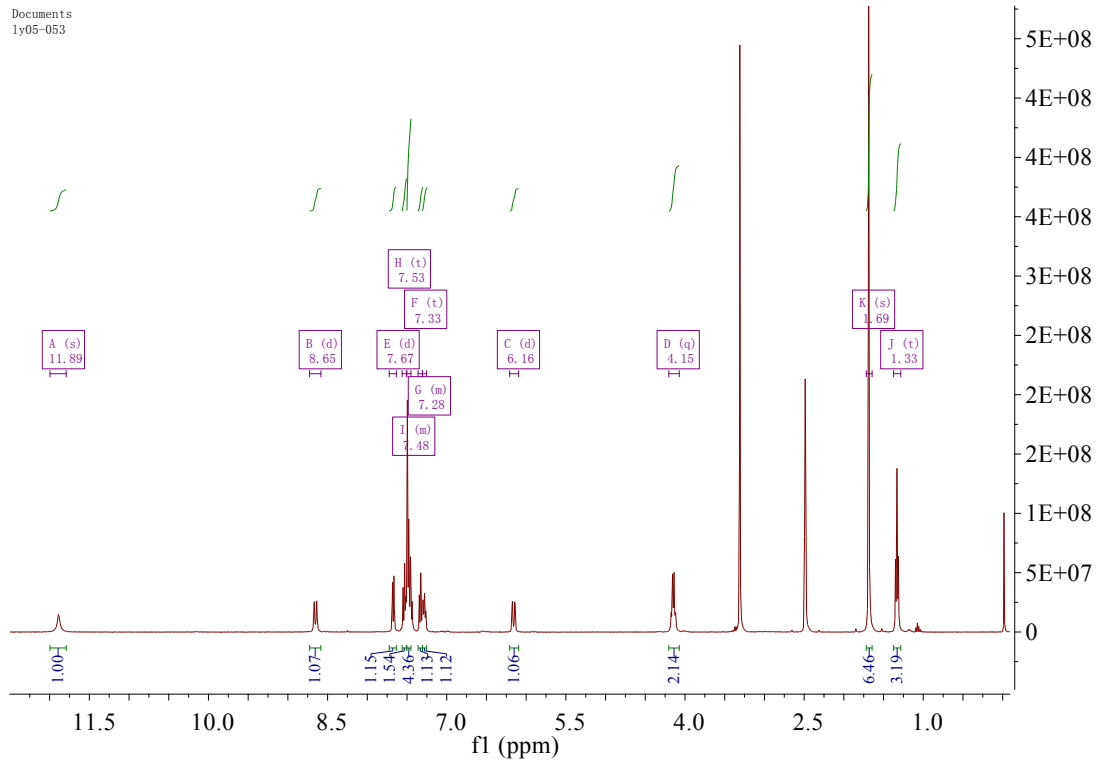

Figure S3. ^{1}H NMR spectrum for compound **2**.

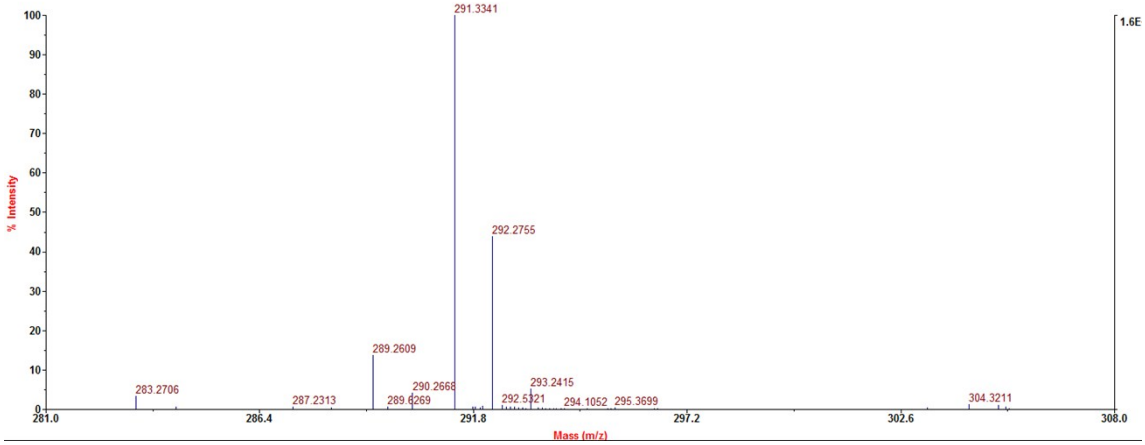

Figure S4. MALDI-TOF-MS spectrum for compound **2**.

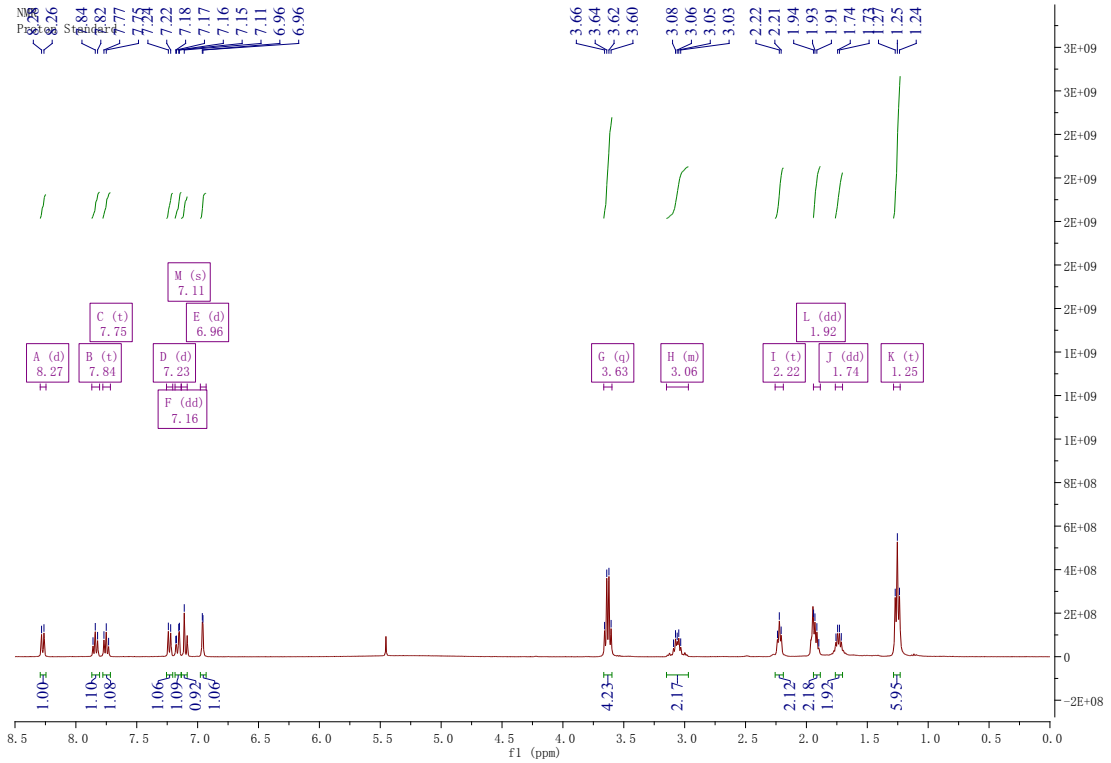

Figure S5. ^{1}H NMR spectrum for compound **3**.

Figure S6. MALDI-TOF-MS spectrum for compound **3**.

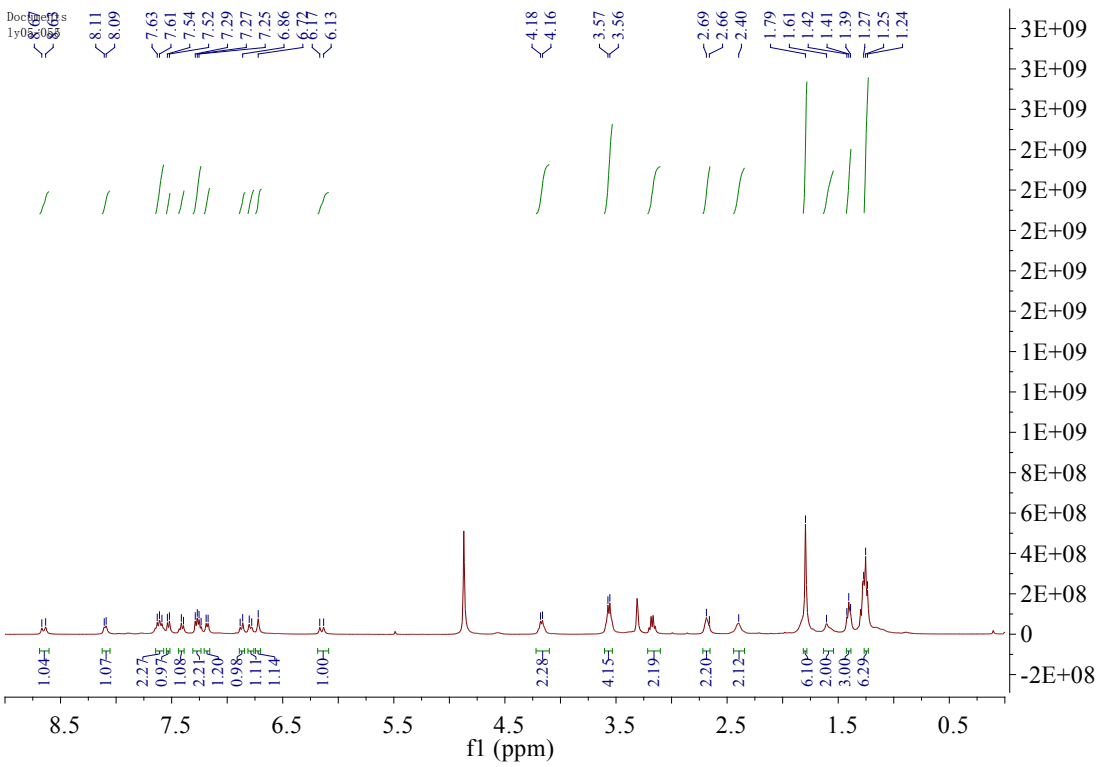

Figure S7. ^{1}H NMR spectrum for compound **NRh-1**.

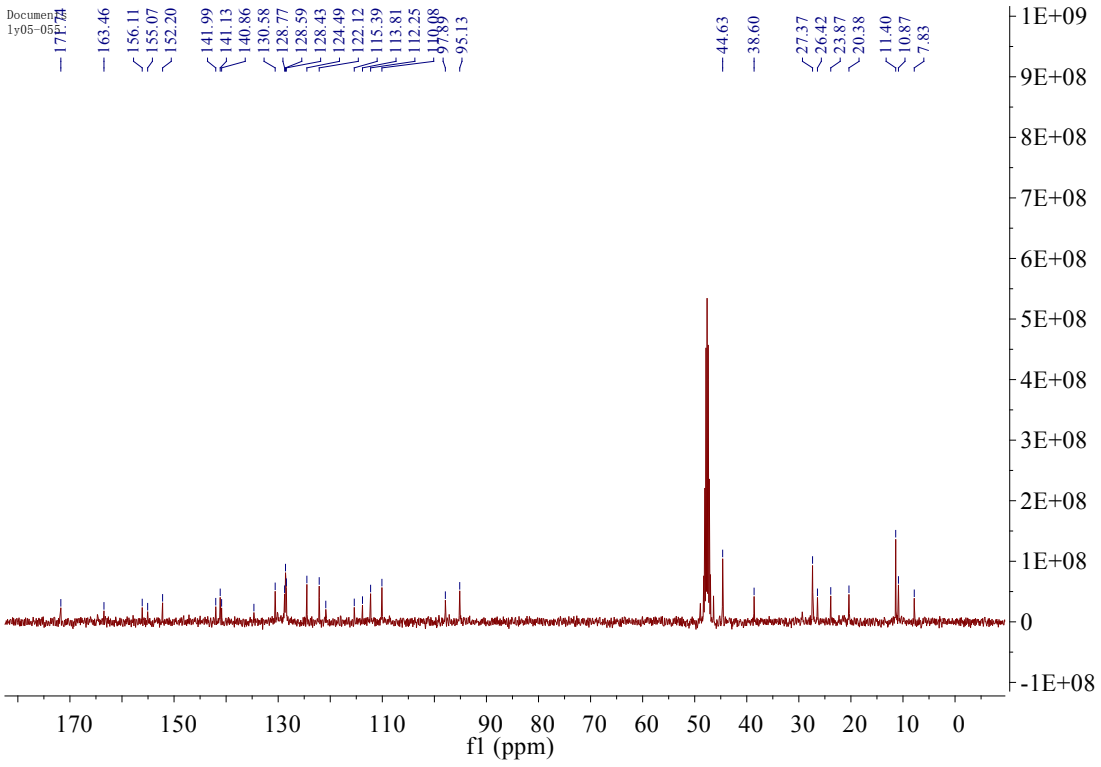

Figure S8. ^{13}C NMR spectrum for compound **NRh-1**.

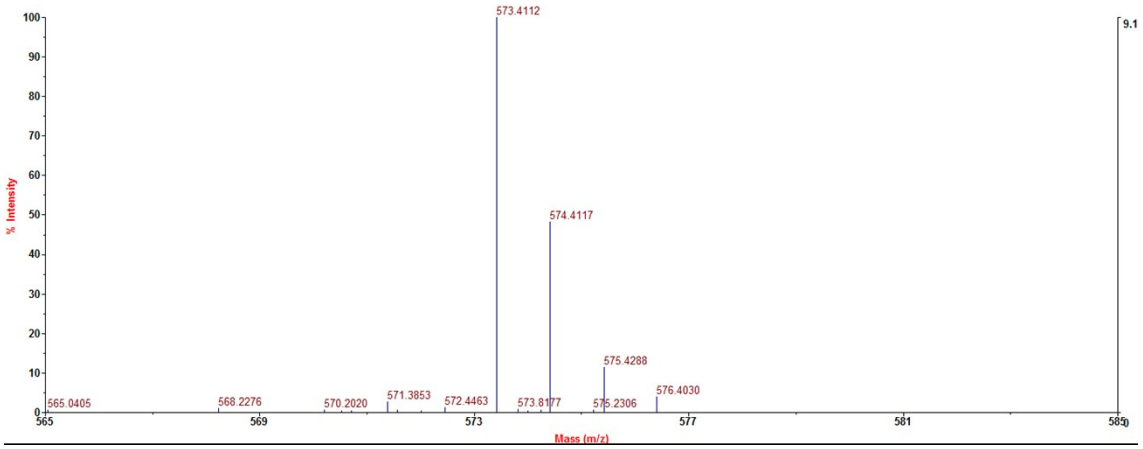

Figure S9. MALDI-TOF-MS spectrum for compound **NRh-1**.

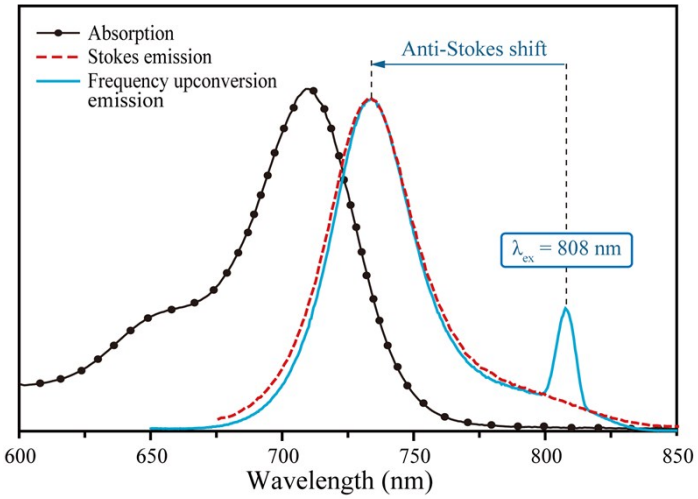

Figure S10. Absorption (black solid), Stokes emission (red dash, λ_{ex} = 670 nm) and anti-Stokes emission spectra of the solution of NRh-1 (5 μM) in EtOH/H_2O (v/v, 1:9).

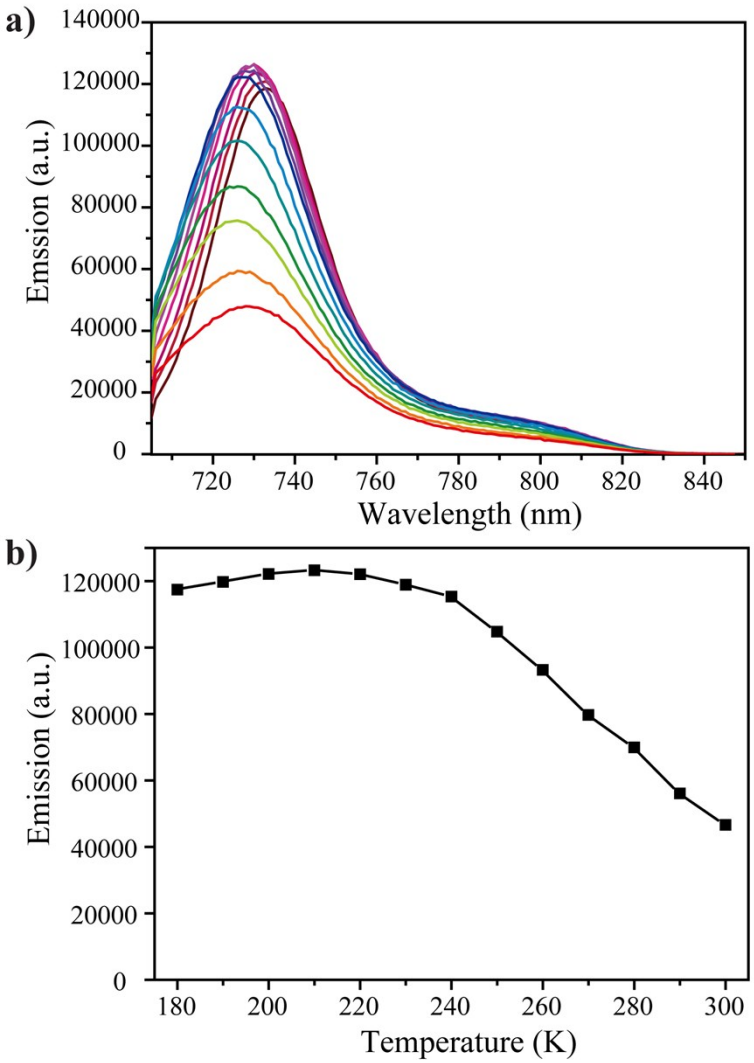

Figure S11. a) The Stokes emission spectra of NRh-1 (5 μM in ethanol) under excitation of 700 nm light at different temperatures (160, 170, 180, 190, 200, 210, 220, 230, 240, 250, 260, 270, 280, 290, and 300K). b) Dependence of fluorescent intensity of NRh-1 at 730 nm on temperature. The traditional Stokes emission occurs mostly from the lowest excited vibrational state S_1 to the vibrational ground state S_0. At higher temperature, the 0←0 vibronic origin of the $S_0 \rightarrow S_1$ electronic transition was reduced, which lead to a decrease in the intensity of Stokes luminescence.

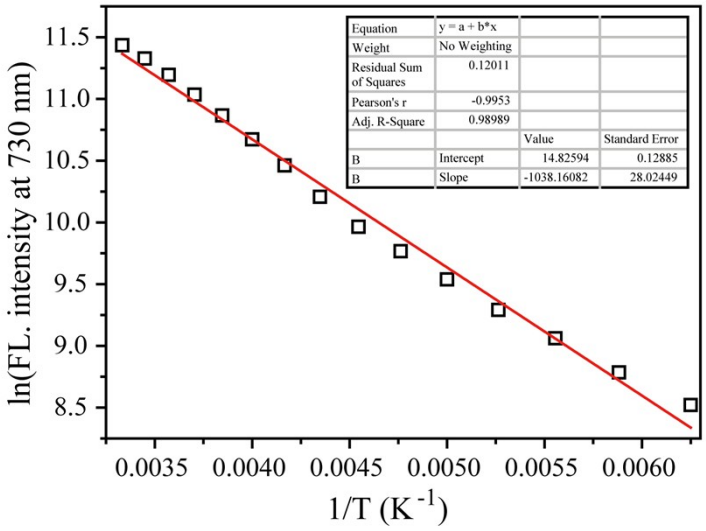

Figure S12. Linear plots of logarithm of fluorescence intensity at 730 nm against inverse temperature (T = 160, 170, 180, 190, 200, 210, 220, 230, 240, 250, 260, 270, 280, 290, and 300 K) of NRh-1 solution. Notably, the detection limit of 0.4 K for temperature can be obtained by using the UCL emission at 730 nm as a detected signal, indicating that NRh-1 could be particularly suitable as temperature probe with high sensitivity.

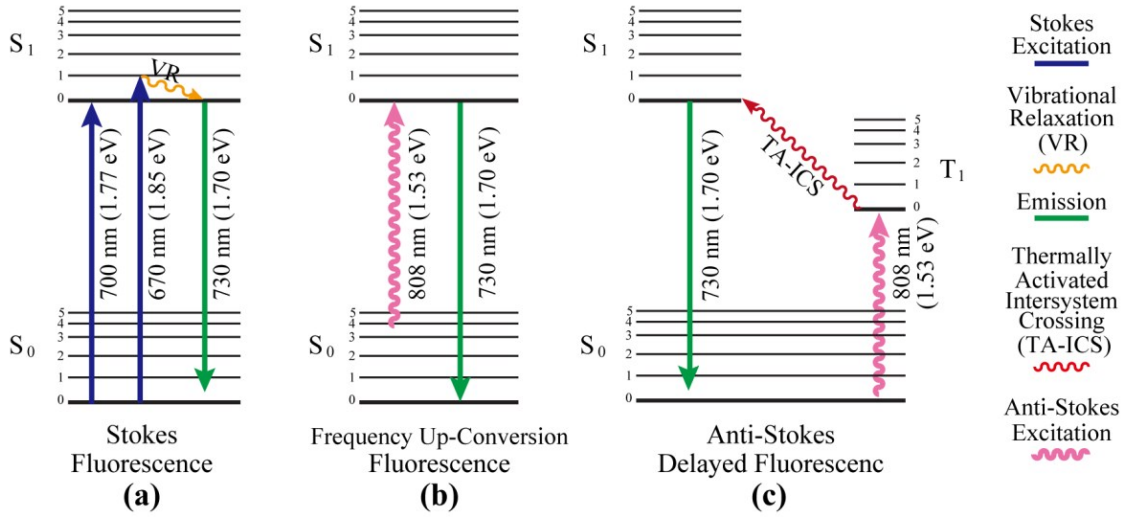

Figure S13. Illustration of the machanisms of Stokes fluorescene (a), frequency upconversion fluorescence (b), and anti-Stokes delayed fluorescence (c) process.

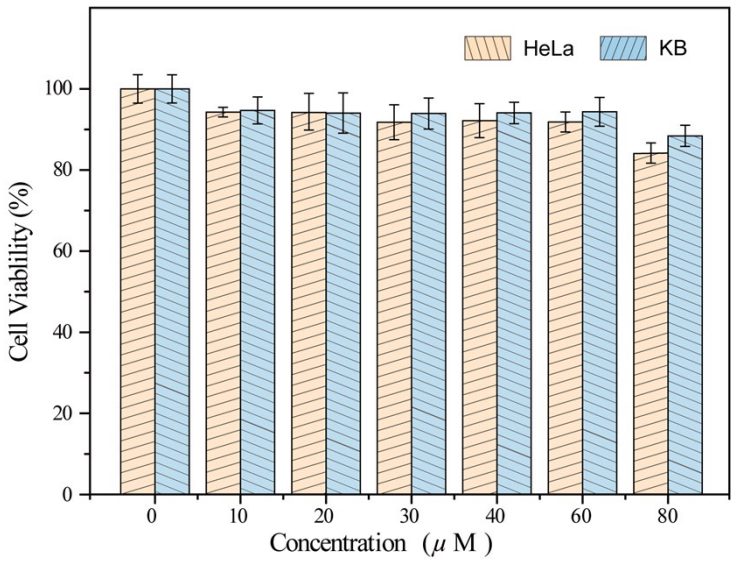

Figure S14. *In vitro* cell viability of HeLa and KB cells incubated with NRh-1 at different concentration for 24 h. To testify the capability of frequency upconversion dye as a biolabel, we undertook in vitro cytotoxicity test by the methyl thiazolyl tetrazolium (MTT) assay. After incubation of 10–80 μM NRh-1 in HeLa and KB cells for 24 h, there is no significant difference in the proliferation of cells was observed, suggesting a low cytotoxicity of NRh-1 toward the incubated cells.

Figure S15. The bright-field, luminescent, and merged images of a living mouse at 5 min post-injection of 40 μL NRh-1, using the NIR UCL emission at 680–750 nm as detected channel. Note: region of interest (ROI) 1, specific uptake; ROI 2, nonspecific uptake; ROI 3, background.

Markably, a high-contrast FUCL in vivo imaging with a high SNR (~24) of living mouse was observed when subcutaneous injected with 40 μL NRh-1 (2.5 μM) in saline. It should be noted that there was no background autofluorescence in the biosamples. The result demonstrated that NRh-1 frequency upconversion dye may be a potential biomarker for *in vivo* labelling and imaging.

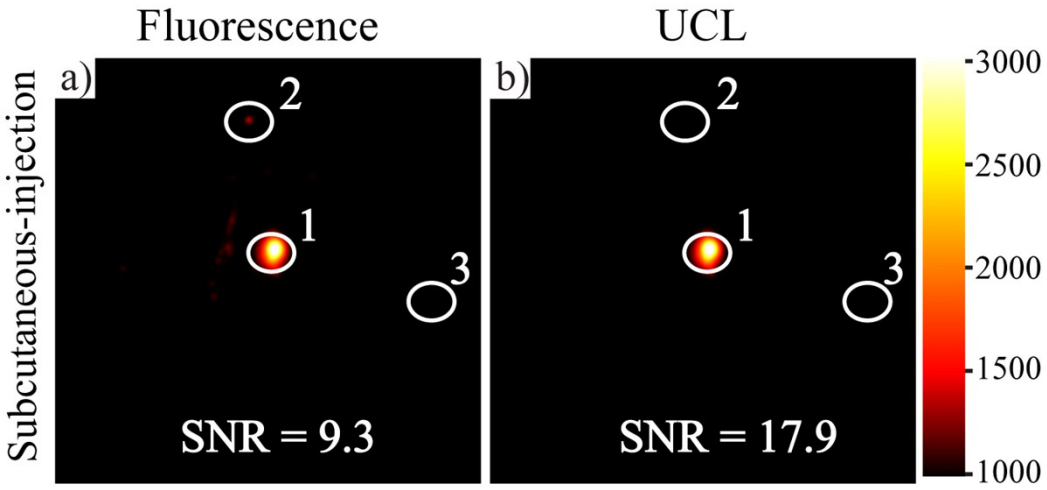

Figure S16. a) The Stokes fluorescence imaging under excitation at 670 nm (5 mW cm^{-2}) and anti-Stokes UCL bioimaging under excitation at 808 nm (20 $mWcm^{-2}$) of a living mouse with subcutaneous (20 μL, 5 μM) injection of NRh-1.

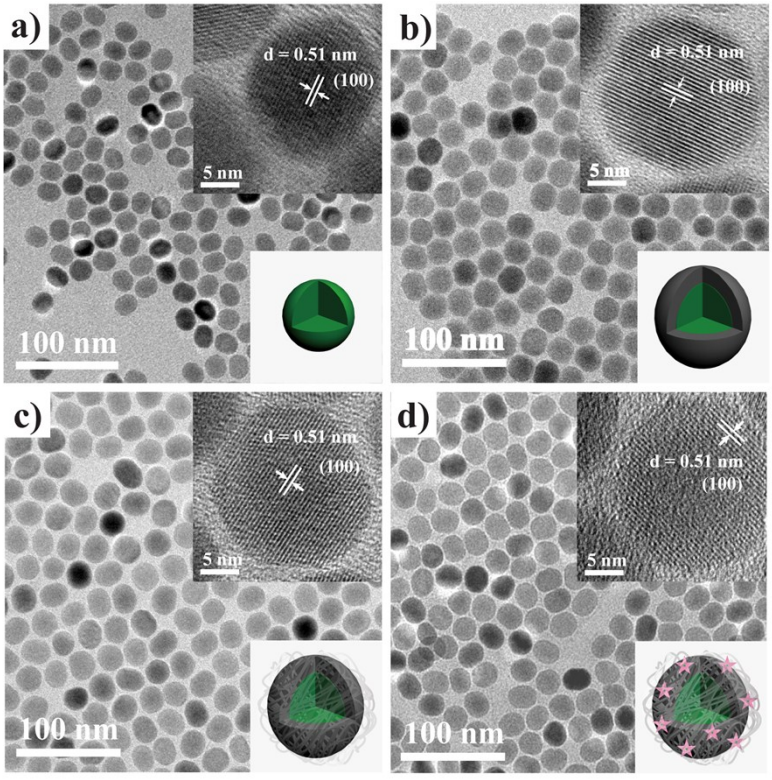

Figure S17. TEM images and HR-TEM images (inset) of OA-UCNPs (a), OA-csUCNP:Nd (b), pPEG-csUCNP:Nd (c), and NRh-1-csUCNPs:Nd (d).

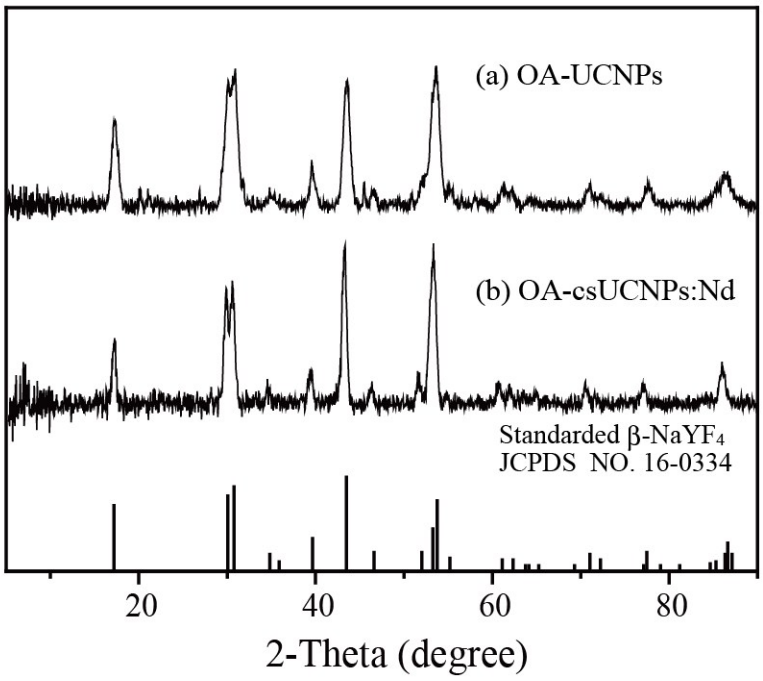

Figure S18. The XRD patterns of the OA-UCNPs (a) and OA-csUCNPs:Nd (b).

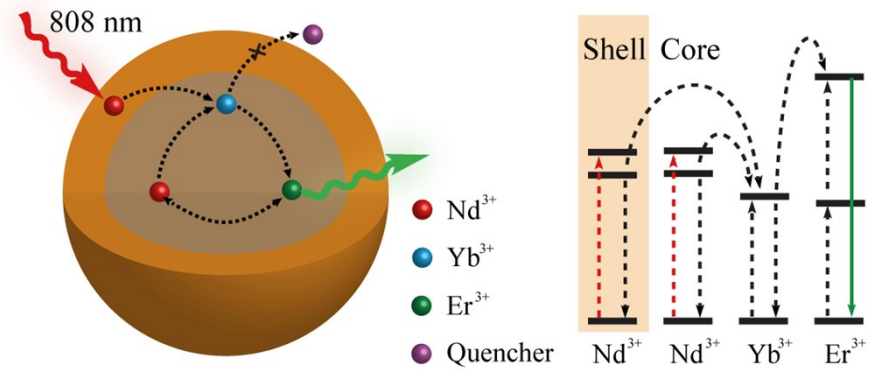

Figure S19. Energy transfer mechanism in csUCNPs:Nd.

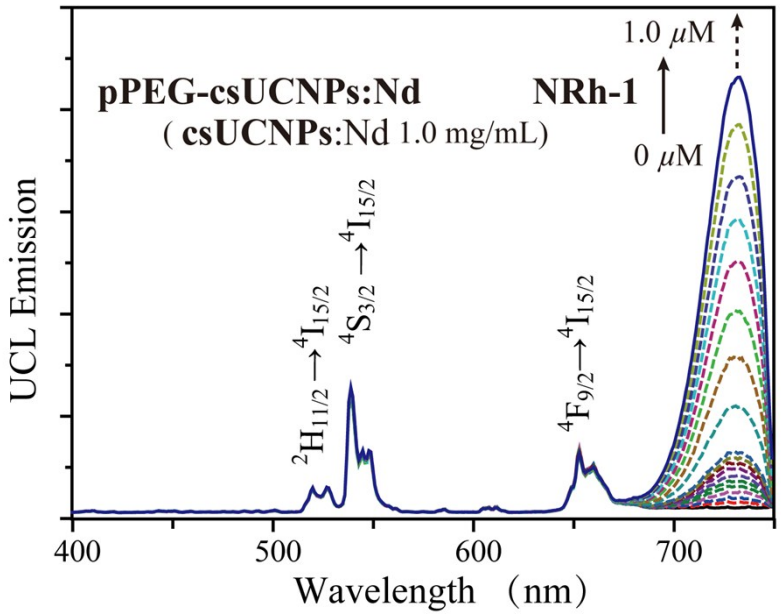

Figure S20. The UCL emission spectra of the mixture of pPEG-csUCNPs:Nd (1.0 mg/mL measured by csUCNPs:Nd) and various amount of NRh-1 (0~1.0 μM) under excitation at 808 nm laser. Note that a short-pass filter at 750 nm was used.

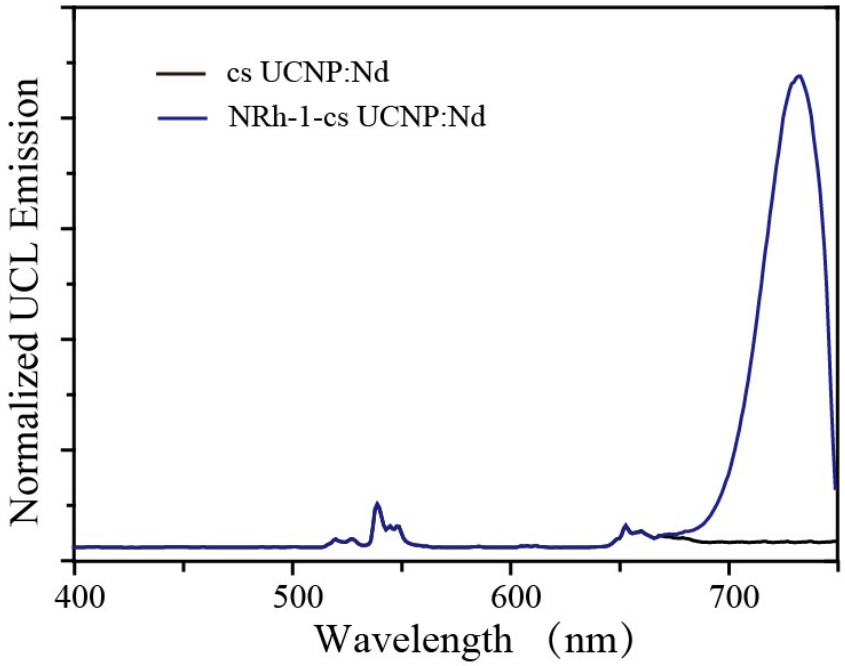

Figure S21. The UCL emission spectra of csUCNP:Nd and NRh-1-csUCNPs:Nd solutions. Note: the emission spectra were normalized at 540 nm. We found that the csUCNP:Nd upconversion emission was not decreased in NRh-1-csUCNP system, indicating that energy transfer from csUCNP:Nd to NRh-1 may not occur in our design.

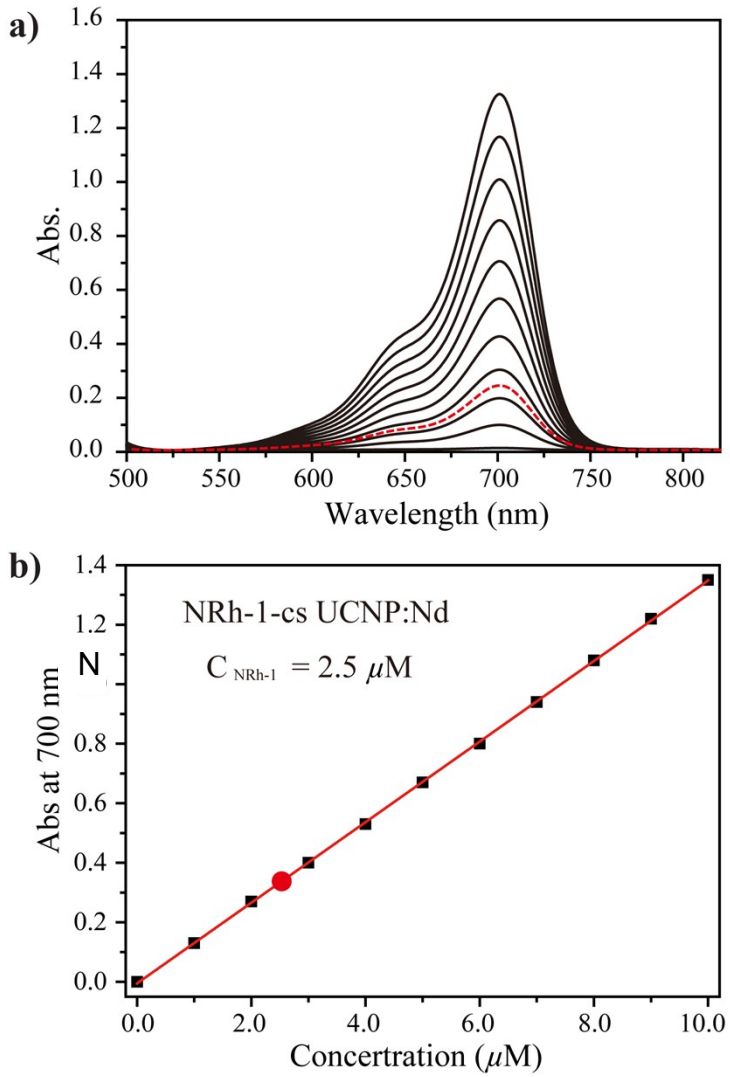

Figure S22. The concentration of NRh-1 loaded in the NRh-1-csUCNPs:Nd was calculated using the absorption spectroscopy technique. a) Absorption spectra of the NRh-1 with different concentrations of 0~10.0 μM. b) The absorbance at 700 nm as a function of NRh-1 concentration. The NRh-1 content (red point) of NRh-1-csUCNPs:Nd (0.5 mg/mL) was determined to be 0.3%. Based on the calculation, approximately 53 NRh-1 molecules were loaded into the surface layer of one upconversion nanoparticles.

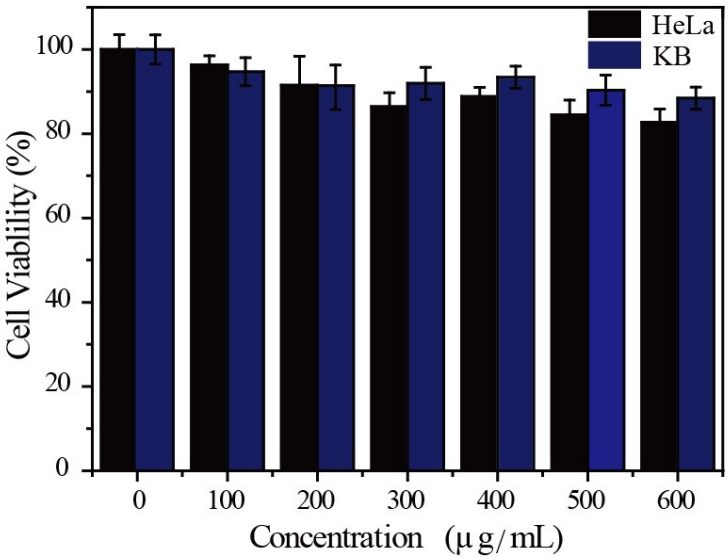

Figure S23. *In vitro* cell viability of HeLa and KB cells incubated with NRh-1-csUCNPs:Nd at different concentrations for 24 h.

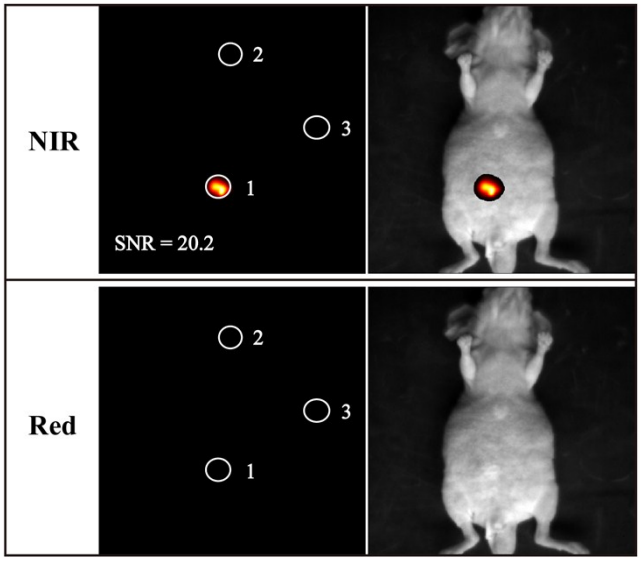

Figure S24. *In vivo* upconversion luminescence imaging of the living mouse at 5 min postinjection of 40 μL NRh-1-csUCNPs:Nd by subcutaneous injection in the NIR (top panel) and red (bottom panel) channels.

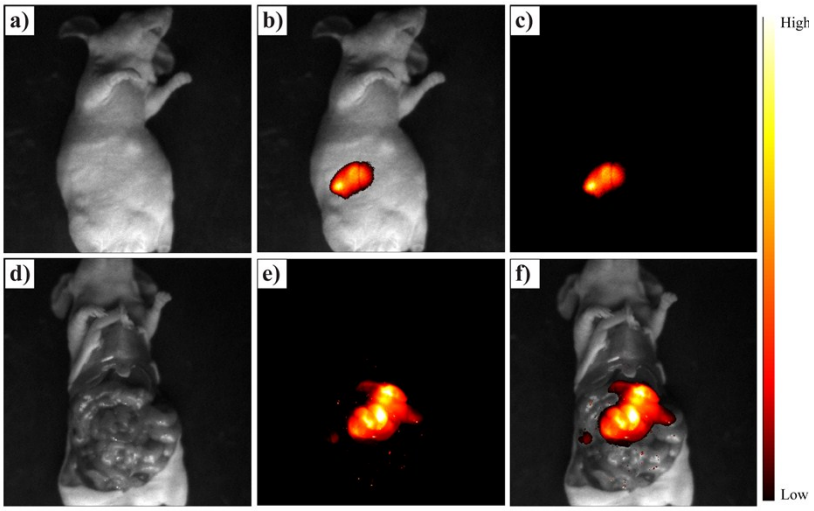

Figure S25. (a-c) *in vivo* and (d-f) *in situ* upconversion luminescence imaging of the living mouse at 5 min postinjection of 100 μL NRh-1 by intragastric administration. (λ_{ex} = 808 nm, λ_{UCL} = 680-750 nm).

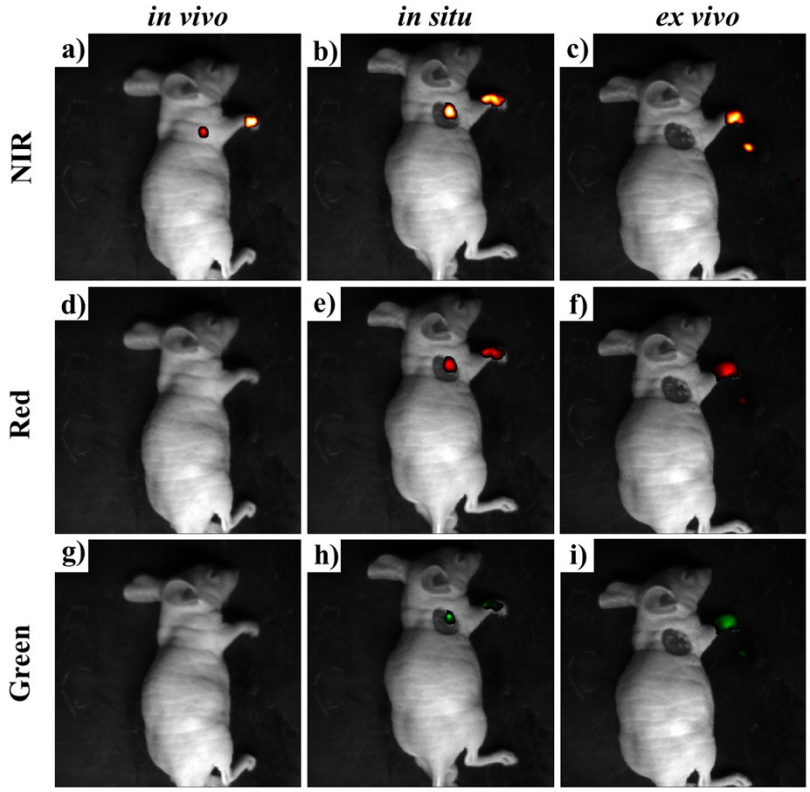

Figure S26. *In vivo* (a, d, g), *in situ* (b, e, h) and *ex vivo* (c, f, i) upconversion luminescence lymphatic imaging of living mouse at 1.0 h postinjection of 40 μL NRh-1-cs UCNPs:Nd, using UCL emissions at 514–560 nm (green channel), 635–680 nm (red channel), or 680–750 nm (NIR channel) as detect signals.

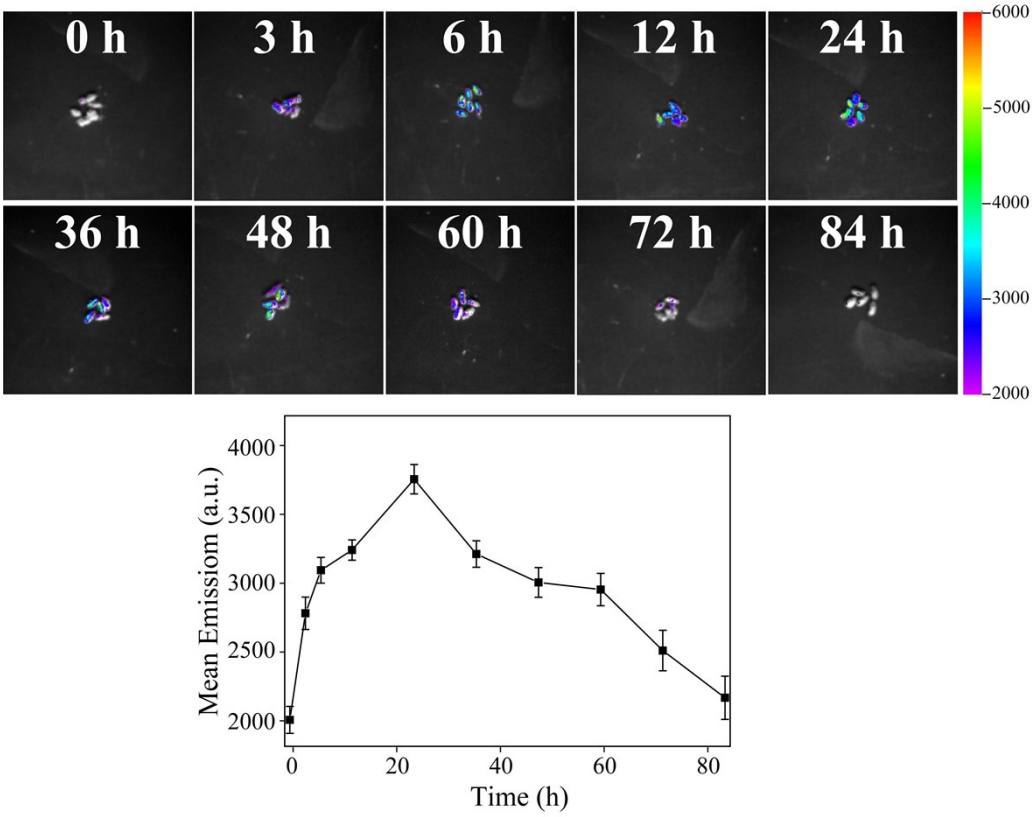

Figure S27. The UCL imaging (top) and the mean emissive intensities (bottom) of the faeces at different time after the treatment with NRh-1.

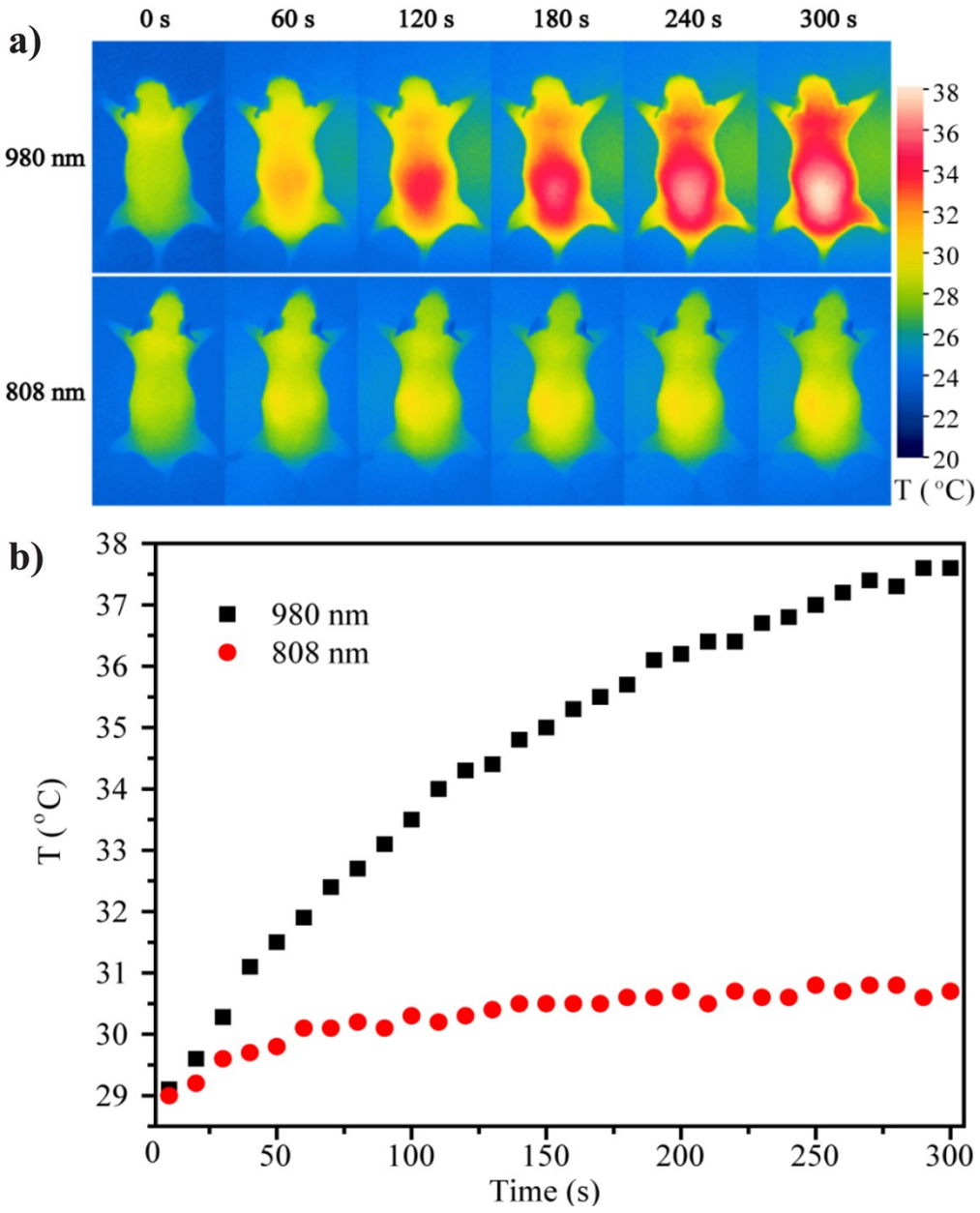

Figure S28. Infrared thermal image (a) and the corresponding measured temperature curve (b) of the nude mice during continuous irradiation with 980 nm or 808 nm laser (power density of *ca*. 100 mW cm^{-2}) for 300 s.

Reference

(1) Guo, Z.; Zhu, W.; Zhu, M.; Wu, X.; Tian, H. *Chem. Eur. J.,* **2010**, *16*, 14424.

(2) Mason, S. J.; Hake, J. L.; Nairne, J.; Cummins, W. J.; Balasubramanian, S. *J. Org. Chem.,* **2005**, *70*, 2939.

(3) Prostota, Y. A. *Chem. Heterocyclic Comp.,* **2004**, *40*, 116.

(4) Xie, X.; Gao, N.; Deng, R.; Sun, Q.; Xu, Q.-H.; Liu, X. *J. Am. Chem. Soc.* **2013**, *135*, 12608.

(5) Liu, Y.; Chen, M.; Cao, T. Y.; Sun, Y.; Li, C. Y.; Liu, Q.; Yang, T. S.; Yao, L. M.; Feng, W.; Li, F. Y. *J. Am. Chem. Soc.* **2013**, *135*, 9869.

(6) Liu, Q.; Yin, B. R.; Yang, T. S.; Yang, Y.; Shen, Z.; Yao, P.; Li, F. Y. *J. Am. Chem. Soc.* **2013**, *135*, 5029.